Journal of Mechanical Science and Technology 29 (7) (2015) 2747~2754
www.springerlink.com/content/1738-494x(Print)/1976-3824(Online)
DOI 10.1007/s12206-015-0603-2

Evaluation and development of improved braking model for a motor-assisted vehicle using MATLAB/simulink †

Sangmyeong Kim[1], Jinsu Kim[1], Gisu Sung[1] and Jinwook Lee[2,*]

[1]*Department of Mechanical Engineering, Graduate School, Soongsil University, Seoul, 156-743, Korea*
[2]*Department of Mechanical Engineering, Soongsil University, Seoul, 156-743, Korea*

(Manuscript Received June 28, 2014; Revised January 22, 2015; Accepted March 24, 2015)

Abstract

In recent years, R&D trends in the automobile industry have involved developing vehicles that are eco-friendly and have good fuel economy in order to meet increasingly stringent vehicle emission and fuel economy regulations. Among various environmentally-friendly vehicles, recently-developed hybrid electric vehicles have been considered a successful technology. To improve the hybrid electric vehicle's efficiency, a regenerative braking system is applied that can save waste braking energy and fuel consumption. To date, much research has been conducted that is related to regenerative brake systems for motor-assisted vehicles. In this study, a vehicle brake model and DC motor model have been developed to predict the braking and electric characteristics of vehicle and motor by using MATLAB/Simulink code and compared with brake performance reference data. Since generating current is a key factor for regenerative braking in a hybrid electric vehicle (HEV) system, electric characteristics are the focus of this study. Therefore, in order to investigate the electric characteristics, analysis is also performed using the DC motor model. The main results obtained by this study are that the vehicle braking dynamics calculated by MATLAB/Simulink simulation were in reasonable agreement with reference values. Using the vehicle brake model, analysis is carried out for investigating the numerical model's characteristics and performances at initial velocity, slip ratio and road conditions. Additionally, experimentation is carried out using a chassis dynamometer and a hybrid electric vehicle, and the data are analyzed.

Keywords: Vehicle brake model; DC motor model; MATLAB/SIMULINK; Regenerative brake system; Current balance; Hybrid electric vehicle

1. Introduction

Recently, R&D trends in the automobile industry have been concentrated on developing vehicles that are eco-friendly and have good fuel economy. These design goals are due to unstable oil costs and more strict regulations on CO_2 and exhaust emission gas. As a result, many developed countries have been focused on designing various automotive powertrains for environmentally-friendly vehicles, including hybrid electric vehicles (HEVs) and alternative fuel vehicles [1, 2]. Among these cars, the hybrid electric vehicle has been considered a successful technology and development of these designs has accelerated in order to address the abovementioned recent issues.

There are many state of the art techniques that improve automotive efficiency, such as regenerative break systems in the case of motor-assisted hybrid electric vehicles. From the perspective of usage of energy, chemical energy from fuel is partially converted to the mechanical energy utilized for vehicles, but the remaining energy is wasted by friction and heat energy when the vehicle slows down. According to some research [3-5], during city driving, approximately 30% of a typical car's engine output is lost to the braking process [3]. Other research has investigated the issue that the conventional spark ignition engine uses only 30% of the fuel energy generated from combustion, while 70% of the fuel energy is dissipated as heat [4]. Other research is related to analyzing the thermal energy dissipated by disc brakes using a simulation process for enhancing the brake efficiency [5]. In motor-driven vehicles, the regenerative braking system is a technology that converts wasted kinetic energy from braking to chemical energy through a battery. When a regenerative braking system operates, the motor serves in the role of generator to collect wasted energy and to reduce energy consumption for the hydraulic brake system. Presently, many studies [6-8] on regenerative braking systems have shown the high potential possibility of these systems in commercial automobiles in order to meet future regulations on emissions and to improve fuel economy. One group investigated a new brake system

*Corresponding author. Tel.: +82 2 820 0929, Fax.: +82 2 820 0650
E-mail address: immanuel@ssu.ac.kr
† Recommended by Associate Editor Eung-Soo Shin

using two motors to control the regenerative brake force and the friction brake force [6]. Interesting research is related to the electrically-controlled regenerative brake system developed for electric passenger vehicles, and vehicles applied the new brake system can reduce energy consumption [7]. Another group investigated the effect of regenerative braking efficiency; fuel consumption was able to be reduced by up to 25% in short-route driving cycles [8].

There are two ways to conduct research on regenerative braking systems. Firstly, using a chassis dynamometer, regenerative braking efficiency can be measured from a test vehicle. This method has an advantage in that practical results are acquired from experimentation with a vehicle. However, the drawback of this method is that an experimental study is time-consuming and requires high initial costs for setup. The other method to conduct the studies on regenerative braking systems is to use numerical simulation code consisting of two designs, for the regenerative braking model and for a vehicle dynamic model. The latter method involves some differences from the practical results obtained from physical experimentation. On the other hand, the low initial costs and ability to adjust various parameters bring huge advantages.

From this perspective, a simulation of a regenerative braking system for a hybrid electric vehicle should be designed to meet the precise prediction of generated current and regenerative energy efficiency. Some interesting research [9-11], is related to simulation of the regenerative braking systems. The projects investigate HEV modeling and simulation for the optimization of various hybrid vehicle configurations and control strategies [9]. Some studies are performed for regenerative braking systems to enhance the energy efficiency and braking performance of the vehicle with simple design and low cost [10]. Other studies have researched the validation of regenerative braking system using hardware in the loop simulation (HILS) and enhancement of the regenerative torque control strategy against booster delay compensation [11].

In this study, numerical simulation with MATLAB/ Simulink was carried out to design a control model of a vehicle braking system to address the most critical part of a HEV model. Then, the model credibility was compared with other models [12]. An analytic model has been applied with the purpose of confirming the electric current generation of a DC motor model driven by a vehicle braking model in order to predict the electric characteristics of the DC motor by using the MATLB/Simulink environment.

2. Numerical procedures

2.1 Vehicle brake model description

Some considerations are specified for simplification purposes. The first condition is that the vehicle moves in a longitudinal direction and force is applied in the horizontal direction. Secondly, the initial instant is considered with null acceleration, resistance of the air, and constant vehicle speed. Finally, the vehicle model is simplified by adapting single-wheel system to investigate the possibility of regenerative braking.

The passive brake type vehicle has been applied with the purpose to develop an analytic model of the vehicle braking system to predict the braking characteristics of the mechanical components by using the MATLAB/Simulink environment, as a unified approach to mechatronic modeling. In order to take into account the braking characteristics of the vehicle in this study, we developed the related analytic model for a vehicle brake model. It consists of numerical simulation code in which each component is represented by an appropriate block and is associated to a mathematical component. The vehicle braking system model was developed to solve the variable equations.

From Newton's second law, we can derive the vehicle dynamic equation, and the vehicle's state at any given time can be determined by solving the equations [12]. In the case of the applied longitudinal force, the force equation of the vehicle can be calculated by the following Eq. (1).

$$M\frac{d^2x}{dt^2}+F_x=0 \tag{1}$$

where M : Mass of the vehicle

F_x : Reactive force of friction

In the case of the normal force, it can be calculated by the following Eq. (2).

$$F_z=Mg\,. \tag{2}$$

Rolling resistance is calculated by normal force. Rolling resistance is simplified and can be expressed as equivalent force acting at the center of the wheel, given by Eq. (3).

$$F_x=\mu_x F_z \tag{3}$$

where μ_x : Rolling resistance coefficient

The μ_x value is a function of many parameters including environmental conditions, vertical loads, surface types, translation speeds and internal pressures of the tires [13]. The Pacejk magic formula is the equation for the longitudinal friction coefficient and the rolling resistance coefficient can be calculated by the following Eq. (4) [14].

$$\mu_x=a(1-e^{-b\lambda}-c\lambda) \tag{4}$$

where λ : Wheel slip ratio

a, b, c : Road condition coefficient

The variables a, b and c can be changed depending on the road surface conditions. We assume that the vehicle is being driven on dry road and wet road conditions.

Fig. 1 shows the correlation between slip ratio and rolling resistance coefficient of dry and wet road conditions. The wheel slip ratio is defined by Eq. (5).

$$\lambda=\frac{v-rw}{v} \tag{5}$$

Table 1. Specifications of the vehicle brake model used in this study.

Vehicle mass (kg)	450
Gravity acceleration (m/s^2)	9.81
Dry road coefficient a, b, c	0.6, 18, 0.52
Wet road coefficient a, b, c	0.15, 40, 0.52
Moment of inertia of tire J_t (kgm^2)	1

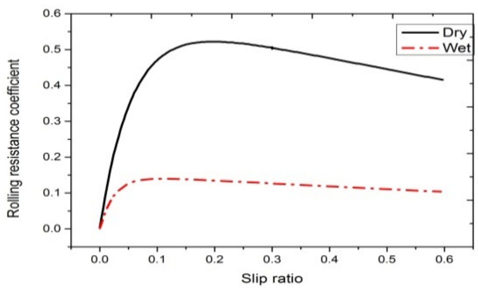

Fig. 1. Correlation between slip ratio and rolling resistance coefficient.

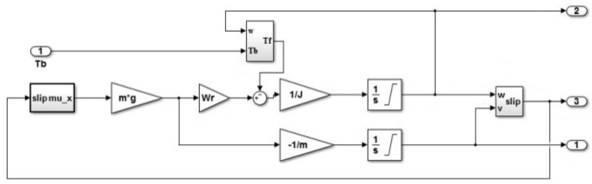

Fig. 2. Vehicle brake model driven by equations used in this study.

where v : Tangent velocity
r : Radius of the wheel
w : Angular velocity of the wheel

The wheel slip is calculated by receiving tangent and angular velocity data from Eq. (1). Additionally, constant slip ratio is controlled by using a PI controller. The moment of the wheel can be calculated by the following Eq. (6).

$$-J_t\frac{d^2\theta}{dt^2}-T_f+F_xr=0 \tag{6}$$

where J_t : Moment of inertia of tire
T_f : Torque of the brake

Fig. 2 shows the vehicle brake model using the composition of the block diagram elaborated for MATLAB/Simulink by applying Eqs. (1)-(6).

2.2 DC motor description

Many electric motors used in hybrid electric vehicles can be categorized as DC (Direct current) motors or AC (Alternating current) motors. Direct current motors have advantages related to smaller volume, the higher speed and power compared AC motor. However, variation in the motoring can be made brush short-lived because it has drawbacks. AC motors offer high efficiency, high power, eases of speed change, and the advantages of long life and low price. However, they involve a disadvantage that the rotation speed is slow [15]. For a variety of reasons, assortments of vehicles are equipped with brushless direct current motors (BLDC), permanent magnet synchronous motors (PMSM) or other forms of motors. In this study, we have researched the DC motor type, including BLDC and PMSM types.

Table 2. Specifications of DC motor model used in this study.

Motor constant B (Nms)	0.1
Motor Kt (Nm/A)	0.41
Back EMF Kv (Vs)	0.25
Inductance L (H)	1.9E-5
Resistance R (ohm)	0.16

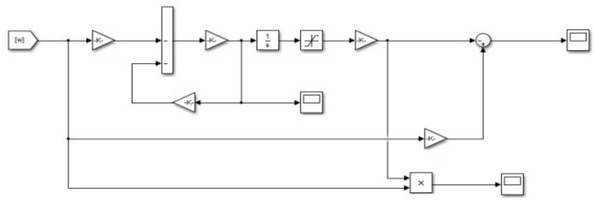

Fig. 3. DC motor model driven by equations used in this study.

The DC motor has been applied with the purpose to predict the electric characteristics of the motor component. The DC motor is modeled as a rotating mass damper system coupled to an electric circuit. In the case of applied rotational torque, the torque equation of the motor can be calculated by the following Eqs. (7) and (8) [16, 17].

$$L\frac{di}{dt}+k_v\omega+Ri=V_{in} \tag{7}$$

$$T_{motor}=k\cdot i \tag{8}$$

where L : Inductance
K_v : Back EMP constant
R : Resistance
V_{in} : Applied voltage constant
k : Generator constant

We can solve for the current applied to the motor's rotor by rearranging to solve the equations and combining T_{motor}.

Fig. 3 shows the DC motor system using the composition of the block diagram, applying Eqs. (7) and (8). "From block", labeled [w], shown in Fig. 3, is an angular velocity input signal from the vehicle braking model. When operating the vehicle brake model and the DC motor model, the vehicle angular speed is multiplied by back EMP constant.

Table 2 shows the specifications of the DC motor model. The parameters of the model were selected by Ref. [17]. Although verifying the data of the DC motor model, the reference did not describe the numerical result data of the generator model. In order to study basic regenerative braking, we have focused on measuring the current produced by the numerical model. In order to confirm the effect on generating current, it was analyzed in terms of the slip ratio and initial vehicle ve-

Table 3. Numerical conditions of the final model used in this study.

Condition	Value
Road condition	Dry road
Slip ratio	0.05, 0.1
Initial velocity (m/s)	16.66 (60 km/h), 25 (90 km/h)

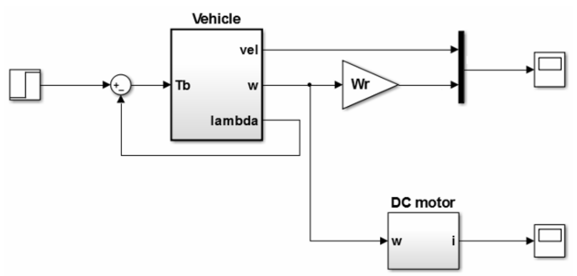

Fig. 4. Main block SIMULINK diagram of vehicle braking model with DC motor model developed by this study.

locity.

Also, the current is multiplied by the motor resistance to determine the drop of voltage. The DC motor model operates with only the input signal of angular velocity from the vehicle brake model. Therefore, the impact on the motor model of V_{in} is negligible. The quantity of voltage is divided by motor inductance. The model can be synchronized to the electrical circuit by introducing a relational expression that generates a current. When the motor rotates, current can be generated by the DC motor model. We have studied the possibility of braking generated by electric current through the braking system.

The final model, which is a combination of the vehicle brake model and the DC motor model, was developed to solve the braking and electric characteristics, as shown in Fig. 4. The step function represents a driver's reaction speed of activating brake when driver want to stop the vehicle setting the response time by 0.2 s. The signals calculated by numerical model can observe a scope that is shown left side in Fig. 4.

2.3 System simulation conditions

Table 3 shows the numerical conditions of the final model used in this study. We select the slip ratio by considering dry and wet road conditions, shown in Fig. 1. As shown, the dry condition's rolling resistance coefficient is the highest value, with a slip ratio of 0.1. Also, as shown, the wet condition's rolling resistance coefficient is the highest value, with a the slip ratio of the 0.05.

3. Result and discussions

3.1 Model verification

Figs. 5 and 8 show the numerical results of the vehicle brake model at the initial velocity of 16.66 m/s, including the comparison of the results with reference data. The vehicle

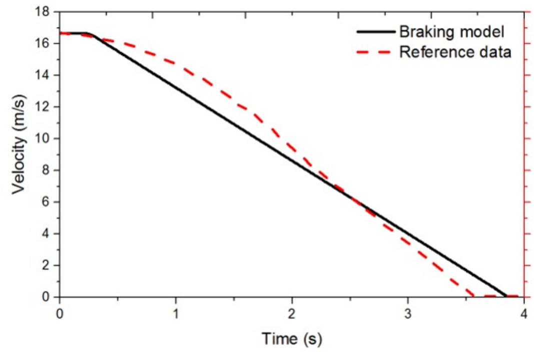

Fig. 5. Vehicle brake model validation for velocity profile.

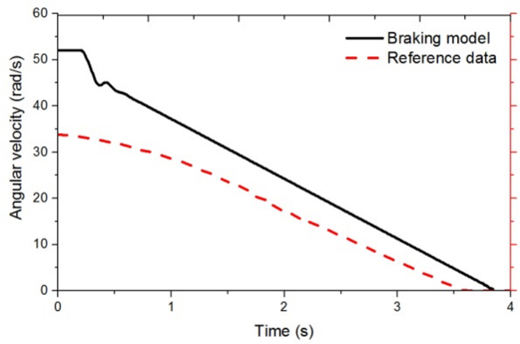

Fig. 6. Vehicle brake model validation for angular velocity profile.

brake model has reported the velocity, angular velocity, acceleration and reaction force. The simulation data is compared with reference data with same figures.

Fig. 5 shows the comparison of velocity between the vehicle brake model and reference data at the initial velocity of 16.66 m/s using the dry road condition. The velocity profile is similar to that of the reference data, even though the vehicle brake model tended to show a late response due to initial brake perception behavior and vehicle's weight.

Fig. 6 shows the verification of angular velocity, and there is a difference between brake model and reference data. The vehicle brake model showed that variation occurs in the first part of the model. The difference was caused that the brake model used the PI controller. Because of the different vehicle weights, the initial angular velocity had a difference value.

Figs. 7 and 8 show the comparisons of acceleration and force between the vehicle brake model and the reference data. The vehicle brake model and reference data display differences among the slope, maximum power and acceleration. The differences are determined by the influence of the difference vehicle weights of the models, and the acceleration and force are exerted relatively rapidly using the control model. The acceleration and force graphs show a similar tendency, despite the differences of the vehicle masses and the controller operating the vehicle brake model.

Fig. 9 shows the effect of the different slip ratios at an initial velocity of 16.66 m/s and using the dry road condition. It is found that the slip ratio conditions have an effect on the brak-

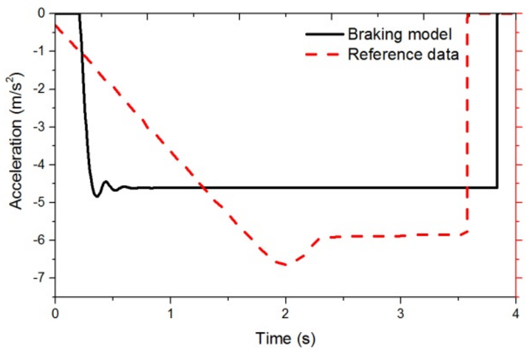

Fig. 7. Vehicle brake model validation for acceleration profile.

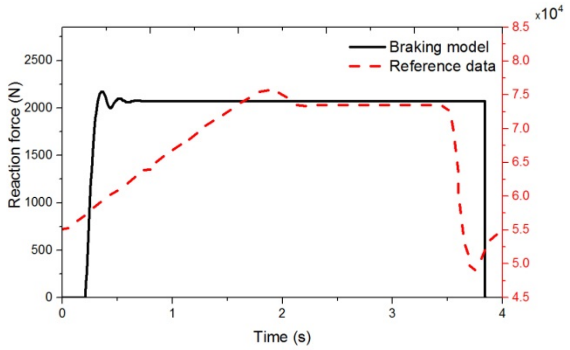

Fig. 8. Vehicle brake model validation for reaction force profile.

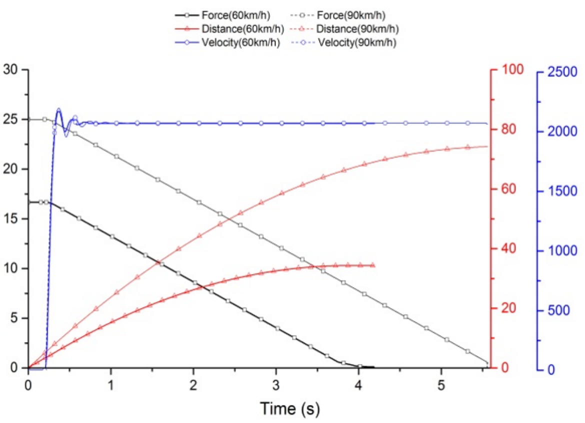

Fig. 9. Effect of different slip ratio at 16.66 m/s (Dry road condition).

ing time, distance and acting force. When the slip ratio is high, braking time and distance are shorter, and braking force is higher than for the low slip ratio. As mentioned above, since the vehicle brake model is controlled by a PI controller whose input is slip ratio, there is an initial difference in the force between 0.1 and 0.05 slip ratio. Because of the different acting forces, the high slip ratio condition has a shorter braking time and distance.

Fig. 10 shows the effect of the different velocities at 0.1 slip ratio and dry road condition. Regardless of the different velocities, it was found that the shapes of the force, distance and velocity trend lines are similar, even though the high initial velocity has an effect on the distance and braking time.

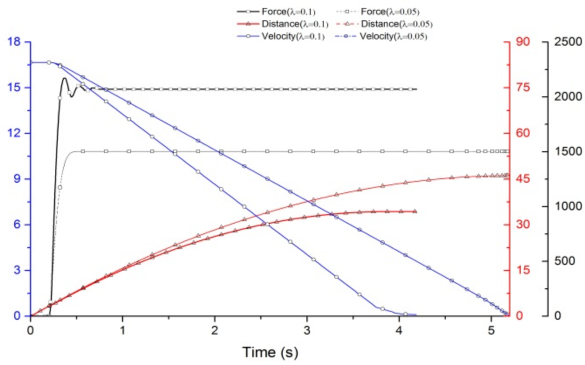

Fig. 10. Effect of different velocities 16.66 m/s and 25 m/s at 0.1 slip ratio (Dry road condition).

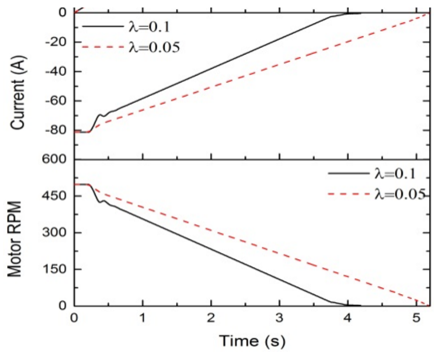

Fig. 11. Electrical effect of different slip ratio at 16.66 m/s (Dry road condition).

3.2 Predicted electric energy solutions

Fig. 11 shows the electrical effect of the different slip ratios at 16.66 m/s and using the dry road condition calculated by the developed model. Comparing on the 0.05 and 0.1 slip ratios, it is found that the increase of braking time has effects on the longer current generation and motor operation at the 0.05 slip condition. Also, it is not affected by the slip ratio to generate the amount of the maximum current, but it is influenced by the initial speed. Since the developed model receives the input signal of the vehicle angular velocity, the amount of the initial current is similar between the 0.05 and 0.1 slip ratios. The most important aspect is observed in the analysis of the current generation and motor operation occurs at the first drastic decreasing wave. It is determined that the effect of the drastic fluctuation is caused to be controlled by the PI controller, as previously discussed.

Fig. 12 shows the electrical effect of different slip ratios at 16.66 m/s and using the wet road condition. Comparing the 0.05 and 0.1 slip ratios, the 0.05 slip condition involves longer-duration motor operation than the 0.1 slip condition. When compared with Fig. 11, the trends of current generation and motor operation appear similar, but the operating time is longer than for the dry road condition.

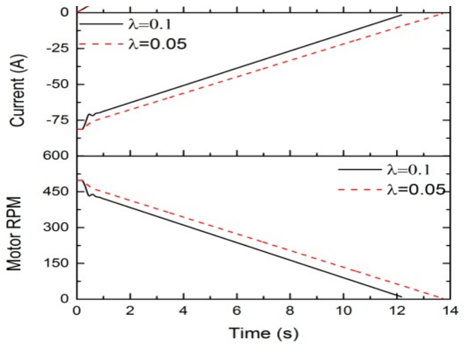

Fig. 12. Electrical effect of different slip ratio at 16.66 m/s (Wet road condition).

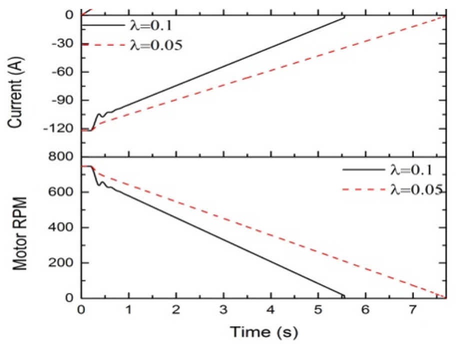

Fig. 13. Electrical effect of different slip ratio at 25 m/s (Dry road condition).

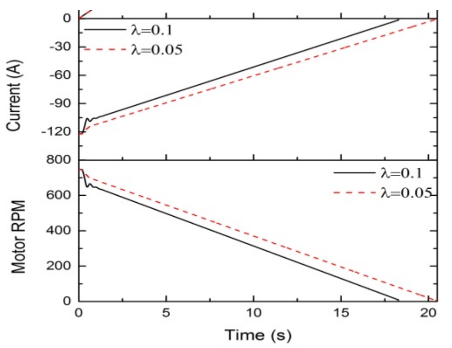

Fig. 14. Electrical effect of different slip ratio at 25 m/s (Wet road condition).

Figs. 13 and 14 show the electrical effect of the different slip ratios and initial velocities for dry and wet road conditions. As shown in Figs. 11 and 12, there are similarities in the electric characteristics over time; the higher slip ratio condition tends to stop more quickly. Also, the wet road condition has a similar tendency to the longer motor operation overall numerical processes. Since Figs. 13 and 14 have higher velocity conditions, however, their initial generating currents represent higher amounts of the current than the 16.66 m/s condition.

In the analysis of the time of motor operation, the slip ratio of the dry road condition has a more significant effect on the time of motor operation than for the wet road condition. When the dry road condition is applied, the 0.1 slip ratio's rolling coefficient is a larger value than the 0.05 slip ratio's rolling coefficient, and there is a large difference value between the 0.05 and 0.1 slip ratios. On the other hand, when the wet road condition is applied, there is little difference of the rolling coefficients at the 0.05 and 0.1 slip ratios, as shown in Fig. 1.

Table 4 represents the results of acting force and generating current with an integrated graph area for the analysis conditions. The amount of force using the braking energy generally showed consistent value at the analysis condition. However, in the case of generating current, the slip value is smaller, the more current is generated because of the low value of the rolling coefficient. Also, it is found that the road condition is more slippery; the more current is generated at different slip ratio and velocity conditions due to having more time for generation.

Table 4. Results of acting force and generating current under analysis conditions.

Road condition	Velocity (km/h)	Slip ratio	Force (Ns)	Current (As)
Dry	60	0.05	7450	-215
		0.1	7450	-153
Wet	60	0.05	7380	-547
		0.1	7440	-467
Dry	90	0.05	11200	-468
		0.1	11000	-329
Wet	90	0.05	11200	-1214
		0.1	11150	-1035

Table 5. Specifications of the vehicle used in this study.

Displacement (cc)	1999
Engine output (hp)	150
Motor output (hp)	40
Transmission	Automatic 6-speed
Drive type	FF

Fig. 15. Photograph of hybrid electric vehicle mounted on chassis dynamometer.

Fig. 15 and Table 5 show the experimental apparatus of the

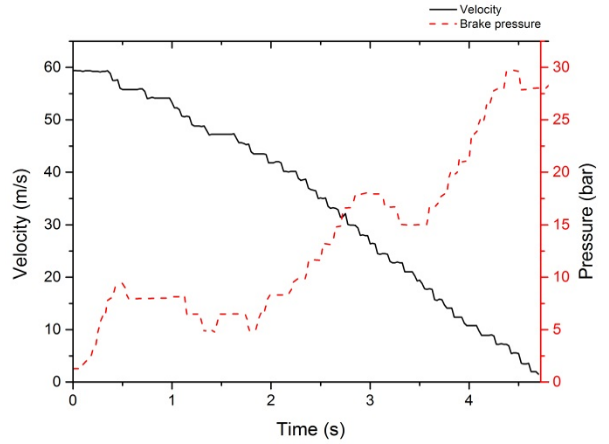

Fig. 16. Experimental data of velocity profile and braking pressure at the initial velocity of 16.66 m/s.

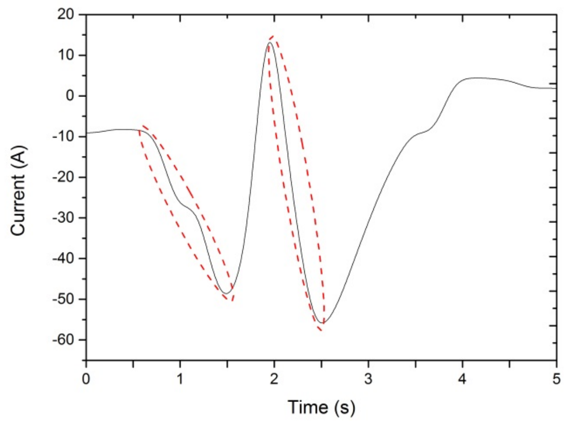

Fig. 17. Experimental data of generating current at the initial velocity of 16.66 m/s.

chassis dynamometer and hybrid electric vehicle in our laboratory. Experimental velocity, braking pressure and current data are acquired by PICO SCOPE and Global diagnostic system (GDS). Since the braking force cannot be acquired by GDS, numerical and experimental data are not compared directly. However, due to the effect of braking pressure on braking force, the data of between braking pressure and force are compared in this study. For comparing the numerical data and experimental data, an experiment was performed at the initial velocity of 16.66 m/s and similar time of operation condition. It can be observed that the experimental data show some fluctuation, presented in Fig. 16, at the velocity and braking pressure due to the roller slip of the chassis dynamometer at the braking moment. The experimental data appear to show fluctuation of the velocity and braking pressure because control is performed by the Hybrid control unit (HCU) and the Transmission control unit (TCU). Fig. 17 shows the generating current data at the same condition. There is a different phase between the numerical and experimental data. The numerical data represent the charging phase at all periods. On the other hands, the experimental data represent the charging and discharging phases. It appears that control by the HCU and TCU affects the results. Because the HCU controls the SOC (State of charge) and regenerative braking system, it was found that the initial SOC has an effect on the experimental current data. Therefore, the numerical model performs analysis of the charging current effect checked dot line area, and confirms the charging effect of generating current at the analysis condition.

4. Conclusions

In this study, a numerical model of a vehicle brake system has been developed to predict the braking characteristics by using the MATLAB /Simulink platform, and has been verified by comparison with the reference data [12]. As a result, it was found that brake performances calculated by MATLAB /Simulink simulation were in reasonable agreement with the reference results. Additionally, the electrical characteristic is confirmed by adding a DC motor model and analyzing the effect of the slip ratio, road condition, and initial velocity for their effects on the generation current. The numerical analysis was conducted and compared with experimental data. The main results concluded from this study are summarized as follows:

(1) Wheel dynamics calculated by the vehicle brake model for considering the conditions among initial velocity, angular velocity, acceleration and force were in reasonable agreement with the reference results.

(2) By comparing the brake characteristics at the different initial velocities, slip ratios and road conditions, it can be observed that a smaller slip ratio provides a longer brake operating time, and that a higher initial velocity requires a effect on the longer brake operating time.

(3) In the DC motor model, the motor rotating the driving mechanism in the vehicle brake model plays an essential role in generating the current at various slip ratios and under different road conditions. Because the generating current is related to the time of motor operation and rolling coefficient, the 0.1 slip ratio's rolling coefficient is a larger value than the 0.05 slip ratio's rolling coefficient. It can be observed that the former has a shorter operating time than the latter, and that the former represents a lower generating current than the latter.

(4) By comparing the results of acting force and generating current, acting force shows a similar tendency at overall conditions . However, in the case of generating current, the smaller the slip value that is represented, the more current that is generated because of the low value of the rolling coefficient. The more slippery the operating conditions, the more current is generated at different slip ratios and velocity conditions due to having a more extended time of generation.

(5) Finally, the study was assessed by the comparison of numerical and experimental data; these showed similar velocity profiles even though there was a difference between the numerical and experimental data. It appears that systems of varying designs produce differences in the associated data.

Acknowledgment

This work was supported by the Royalty program(10045650, Development of analytic process and characteristic analysis of powertrain by constructing power measurement system for high-efficiency parallel hybrid electric vehicle) funded by the Ministry of Trade, industry & Energy(MOTIE, Korea).

References

[1] T. Ueda and A. Ohata, Trends of future power-train development and the evolution of power-train control systems, *SAE Technical Paper*, *SAE 2004-21-0063* (2004).

[2] Y. Kuze, H. Kobayashi, H. Ichinose and T. Othuka, Development of new generation hybrid system (THSⅡ) - development of Toyota coolant heat storage system -, *SAE Technical Paper*, *SAE 2004-01-0643* (2004).

[3] K. Zheng, Y. Yao, T. Shen, K. Hikiri and M. Sasaki, Modeling and control of regenerative braking system in heavy duty hybrid electrical vehicles, *SAE Technical Paper*, *SAE 2008-01-1569* (2008).

[4] T. Noyori, S. Komada and H. Awakawa, Development of a new regenerative braking system, *SAE Technical Paper*, *SAE 2013-32-9006* (2013).

[5] P. Hwang, X. Wu and Y. Jeon, Repeated brake temperature analysis of ventilated brake disc on the downhill road, *SAE Technical Paper*, *SAE 2008-01-2571* (2008).

[6] E. Nakamura, M. Soga, A. Sakai, A. Otomo and T. Kobayashi, Development of electronically controlled brake system for hybrid vehicle, *SAE Technical Paper*, *SAE 2002-01-0300* (2002).

[7] J. Zhang, L. Chen, X. Yue and M. Qiu, Development of the electrically-controlled regenerative braking system for electrified passenger vehicle, *SAE Technical Paper*, *SAE 2013-01-1463* (2013).

[8] C. Albrichsfeld and J. Karner, Brake system for hybrid and electric vehicles, *SAE Technical Paper*, *SAE 2009-01-1217* (2009).

[9] S. Khastgir and P. Warule, Regenerative braking strategy for an unaltered mechanical braking system of a conventional vehicle converted into a hybrid vehicle, *SAE Technical Paper*, *SAE 2013-26-0155* (2013).

[10] H. E. Ahu, U. M. C. Ismail, S. Volkan, G. Levent, A. Tankut, K. Varlik and Y. Murat, Electric regenerative power assisted brake algorithm for a front and rear wheel drive parallel hybrid electric commercial van, *SAE Technical Paper*, *SAE 2008-01-2606* (2008).

[11] K. Bayar, M. Ryan, H. Yu and C. Dale, Regenerative braking control enhancement for the power split hybrid architecture with the utilization of hardware-in-the-loop simulations, *SAE Technical Paper*, *SAE 2013-01-1466* (2013).

[12] F. F. H. B. Joao, A. P. Eduardo and A. E. M. Jose, Design of a pneumatic regenerative braking system, *SAE Technical Paper*, *SAE 2005-01-3969* (2005).

[13] Goddard Consulting, *Software tutorial* (2013).

[14] H. B. Pacejka, *Tyre and vehicle dynamics*, Society of Automotive Engineering and Butterworth-Heinemann, Oxford (2002).

[15] Y. W. Jeong and G. S. Jeong, *Electric vehicle*, GS Intervision, Seoul, Korea (2011).

[16] Y. G. Shin, *Automatic control systems engineering*, Second Ed. Intervision, Seoul, Korea (2007).

[17] K. Burak and B. Melody, Developing an extensible and concise Simulink toolset for hybrid vehicle modeling and simulation, *SAE Technical Paper*, *SAE 2011-01-0755* (2011).

Sangmyeong Kim received his Master's degree in Mechanical Engineering, Soongsil University, Korea. He is currently a Ph.D. student at Center for Power Source Research for Next-Generation Mobility of Chiba University, Japan. His research interests are powertrain and vehicle emission technology of diesel and gasoline vehicles using chassis dynamometer and PEMS.

Jinwook Lee received his Ph.D. in Mechanical Engineering, Seoul National University, Korea. He is currently a professor at department of mechanical engineering, Soongsil University. His research interests are automotive powertrain system and clean energy technology for ICV, HEV and FCEV.